



Originally published as:

Usoskin, I. G., Mironova, I. A., Korte, M., Kovaltsov, G. A. (2010): Regional millennial trend in the cosmic ray induced ionization of the troposphere. - *Journal of Atmospheric and Solar-Terrestrial Physics*, 72, 1, 19-25,

DOI: [10.1016/j.jastp.2009.10.003](https://doi.org/10.1016/j.jastp.2009.10.003)

Manuscript Number:

Title: Regional millennial trend in the cosmic ray induced ionization of the troposphere

Article Type: Research Paper

Keywords: Paleomagnetism; Cosmic rays; Atmosphere; Climate

Corresponding Author: Dr. Ilya Usoskin,

Corresponding Author's Institution: University of Oulu, Sodankylä Geophysical Observatory

First Author: Ilya Usoskin

Order of Authors: Ilya Usoskin; Irina A Mironova, Ph.D.; Monika Korte; Gennady A Kovaltsov

Abstract: Long-term trends in the tropospheric cosmic ray induced ionization on the multi-millennial time scale are studied using the newly released paleomagnetic reconstruction models. Spatial and temporal variations of the tropospheric ionization has been computed using the CRAC:CRII model and applying the paleomagnetic CALS7k.2 reconstruction. It has been shown that long-term variations of the tropospheric ionization are not spatially homogeneous, and they are defined not only by solar (i.e., covariant with solar irradiance) changes but also by the geomagnetic field. The dominance of the two effects is geographically separated, which makes it possible to distinguish between direct and indirect solar-terrestrial climate effects. Possible climate applications are considered.

Regional millennial trend in the cosmic ray induced ionization of the troposphere

I.G. Usoskin^{*,a}, I.A. Mironova^b, M. Korte^c, G.A. Kovaltsov^d

^a*Sodankylä Geophysical Observatory (Oulu unit), 90014 University of Oulu, Finland*

^b*Institute of Physics, St. Petersburg State University, Russia*

^c*Helmholtz Centre Potsdam, GFZ German Research Centre for Geosciences, Potsdam, Germany*

^d*Ioffe Physical-Technical Institute, St. Petersburg, Russia*

Abstract

Long-term trends in the tropospheric cosmic ray induced ionization on the multi-millennial time scale are studied using the newly released paleomagnetic reconstruction models. Spatial and temporal variations of the tropospheric ionization has been computed using the CRAC:CRII model and applying the paleomagnetic CALS7k.2 reconstruction. It has been shown that long-term variations of the tropospheric ionization are not spatially homogeneous, and they are defined not only by solar (i.e., covariant with solar irradiance) changes but also by the geomagnetic field. The dominance of the two effects is geographically separated, which makes it possible to distinguish between direct and indirect solar-terrestrial climate effects. Possible climate applications are considered.

Key words: Paleomagnetism, Cosmic rays, Atmosphere, Climate, Holocene,

1. Introduction

2 During the pre-industrial epoch, influence of outer space factors on the
3 terrestrial climate may be significant. Most apparent external climate drivers
4 are related to the orbital forcing, resulting in the changing insolation, which
5 can be straightforwardly included into paleoclimatic studies (e.g., Haigh

*Corresponding author

Email address: ilya.usoskin@oulu.fi (I.G. Usoskin)

6 et al., 2005). Possible relations between solar variability and climate on
7 multi-millennial time scale are intensively discussed but their causes are not
8 resolved (e.g., Bond et al., 2001; Xiao et al., 2002; Hong et al., 2001; Nigge-
9 mann et al., 2003; Haigh et al., 2005; Bard and Frank, 2006). In particular,
10 large uncertainties remain in reconstructions of the long-term solar irradiance
11 (total or spectral) and its effect upon climate (e.g., Haigh et al., 2005; Foukal
12 et al., 2006). Another important factor of the outer space influence upon the
13 terrestrial environment is formed by cosmic rays (e.g., Dorman, 2004; Usoskin
14 and Kovaltsov, 2008). Cosmic rays (CR) are often considered as simply in-
15 verted solar activity, due to the heliospheric modulation. However, this is
16 true only on a relatively short time scale, shorter than a century. On longer
17 scales, centennial to millennial, CR flux at the Earth is greatly affected also
18 by changes of the geomagnetic field (e.g., Christl et al., 2004; Usoskin et al.,
19 2008) or, at geological time scales, even by the changing galactic surrounding
20 (Scherer et al., 2006). Accordingly, variations of CR in the Earth's atmo-
21 sphere can be essentially different from solar activity on longer time scales,
22 leading to potentially distinguishable effects on the terrestrial environment.
23 In this context, variations of the geomagnetic field and the ensuing CR varia-
24 tions are sometimes considered as an independent possible external driver for
25 the climate (cf. Gallet et al., 2005, 2006; Hyodo et al., 2006; Courtillot et al.,
26 2007; Kitaba et al., 2009; Knudsen and Riisager, 2009). In this paper we
27 emphasize that separating different outer factors may shed new light on our
28 understanding of the natural external drivers of the pre-industrial climate.

29 The most important terrestrial effect of CR is related to the ionization
30 of the ambient air (Bazilevskaya et al., 2008), which is called the cosmic ray
31 induced ionization (CRII). Cosmic rays form the main source of ionization
32 in the low-to-middle atmosphere, and therefore their variability directly af-
33 fects such atmospheric conditions as ion concentration and conductivity. On
34 the other hand, these direct atmospheric effects may result in further at-
35 mospheric changes, which are potentially capable of affecting climate. Such
36 potential mechanisms include enhanced aerosol and cloud formation in the
37 troposphere, mediated by CR (see, e.g., Marsh and Svensmark, 2003; Scherer
38 et al., 2006; Kazil et al., 2006, 2008; Arnold, 2008; Mironova et al., 2008; Tins-
39 ley, 2008). Although details of these mechanisms remain unclear, giving rise
40 to some scepticism (e.g., Bard and Frank, 2006), it could be expected that
41 enhanced CRII would correspond to a larger amount of tropospheric clouds,
42 and thus to colder and wetter regional climate. This link may be partly
43 responsible for the long-term solar-climate influence (e.g., Van Geel et al.,

44 1999; de Jager, 2005; Versteegh, 2005), in concurrence with other solar fac-
45 tors, such as total or spectral solar irradiance (e.g., Haigh and Blackburn,
46 2006).

47 It has been discussed (Marsh and Svensmark, 2003; Pallé et al., 2004;
48 Usoskin et al., 2006; Voiculescu et al., 2006) that the relation, if existing,
49 between different types of cloud and CRII has clear regional dependence and
50 can be hardly presented as an overall global link, especially on the annual
51 to decadal time scales. On the other hand, long-term (centennial) changes
52 in CRII can also be different in different regions, affected by the fast geo-
53 magnetic axis migration (Kovaltsov and Usoskin, 2007; Usoskin et al., 2008).
54 In this paper we study regional changes of the tropospheric CRII over the
55 last 6–7 millennia and show the importance of the geomagnetic field vari-
56 ations. We also provide, as a possible implication of the millennial CRII
57 regional variations, a statistical comparison between regional paleo-climatic
58 (lake status) reconstructions and the computed tropospheric CRII variations.
59 Such a study may shed a new light on the role, if any, of cosmic rays on the
60 long-term regional climate variations.

61 Here we concentrate on the long-term studies for the pre-industrial epoch
62 without essential anthropogenic factors. We note that any advance in the
63 knowledge of natural external climate forcing may lead to a progress in our
64 understanding of the man-made effects during the modern epoch.

65 2. Cosmic Ray Induced Ionization

Cosmic rays, mostly of galactic origin, are highly energetic particles, per-
manently impinging upon the Earth’s atmosphere. They initiate a compli-
cated nucleonic-electromagnetic cascade in the atmosphere, which can affect
its physical-chemical conditions. Cosmic ray induced ionization is a result
of the cascade induced by energetic cosmic rays in the Earth’s atmosphere.
The ionization rate at a given location and altitude h can be expressed as
(Usoskin et al., 2004):

$$Q = \sum_i \int_{T_{c,i}}^{\infty} J_i(T, \phi) Y_i(h, T) dT, \quad (1)$$

66 where summation is over different species of primary CR, J_i is the differential
67 energy spectrum of the i^{th} specie of CR near Earth outside the geomagnetic
68 field, and $Y_i(h, T)$ is the ionization yield function. Integration is over the

69 kinetic energy T above $T_{c,i}$, which is the kinetic energy corresponding to the
70 local vertical geomagnetic cutoff rigidity P_c . Assuming the constancy of the
71 chemical composition and physical properties of the atmosphere, one can
72 see that the CRII temporal variations (at a given altitude) are controlled
73 by two mutually independent factors: local geomagnetic cutoff, defined by
74 the geomagnetic field; and differential energy spectrum of CR outside the
75 magnetosphere. In this study we use CRII as computed by a CRAC (Cosmic
76 Ray induced Atmospheric Cascade) full 3D numerical model (Usoskin and
77 Kovaltsov, 2006), whose validity for the troposphere and stratosphere has
78 been verified in different conditions (Usoskin et al., 2009). The CRAC:CRII
79 model computes CRII at a given altitude as function of the CR energy spec-
80 trum, parameterized via the heliospheric modulation potential ϕ , and the
81 local geomagnetic rigidity cutoff P_c .

82 Since the interstellar CR spectrum can be regarded as constant on the
83 millennial time scale (Scherer et al., 2006), all changes in the CR spectrum
84 near Earth are ascribed to the modulation of CR in the heliosphere, ulti-
85 mately determined by the solar magnetic activity (Usoskin and Kovaltsov,
86 2004). For long-term studies it is common to parameterize the CR energy
87 spectrum using the only time variable parameter, the modulation potential
88 ϕ , in the framework of the force field approximation (see the full formalism in
89 Usoskin et al., 2005b). Here we use a recent reconstruction of the modulation
90 potential over the last 7000 years from the data on cosmogenic ^{14}C (Usoskin
91 et al., 2007). This reconstruction is based on the same paleomagnetic model
92 CALS7K.2 as we use here, thus minimizing possible systematic errors due
93 to uncertainties of the geomagnetic field reconstruction. The temporal vari-
94 ability of the reconstructed modulation potential since 4000 BC is shown in
95 Fig. 1A. The long-term trend in the solar modulation of CR was negative,
96 the modulation being gradually decreasing between 2000 BC and the Spörer
97 minim of solar activity ca. 1500 AD. The modulation was quickly increasing
98 since the Maunder minim ca. 1700 AD until present, but this plays only a
99 little role in the multi-millennial trend.

Shielding effect of the geomagnetic field hampers CR particles from reach-
ing the atmosphere (e.g., Smart et al., 2000; Kudela and Usoskin, 2004). In
a simple form, well suitable for long-term studies, the geomagnetic shielding
can be parameterized via the geomagnetic cutoff rigidity P_c , which implies a
low bound of rigidity a CR particle must possess in order to reach the atmo-
sphere (Cooke et al., 1991). Most important for the geomagnetic shielding
is the dipole component of the magnetic field, since higher moments decay

more rapidly with distance from the source. In the dipole approximation, the geomagnetic vertical cutoff rigidity is evaluated using the Störmer’s equation (Elsasser et al., 1956):

$$P_c \approx 1.9 \cdot M \left(\frac{Ro}{R} \right)^2 \cos^4 \lambda_G, \quad (2)$$

100 where M is the geomagnetic dipole moment (in 10^{22} A m²), Ro is the Earth’s
 101 mean radius, and R and λ_G are the distance from the given location to the
 102 dipole center and the angular distance to the magnetic pole (geomagnetic
 103 latitude), respectively, and P_c is expressed in GV. Here we use a model of the
 104 eccentric dipole, which takes into account the quadrupole contributions from
 105 a standard spherical harmonic description and is a good approximation to the
 106 reality at the relevant distance from the Earth (Webber, 1962; Fraser-Smith,
 107 1987). The eccentric dipole has the same dipole moment and orientation of
 108 the axis as the centered dipole, but the center of the dipole and consequently
 109 the poles defined as the points where the axis crosses the surface are shifted
 110 with respect to the geographical ones. The first eight Gauss coefficients of
 111 a geomagnetic field model are necessary to compute the dipole moment M ,
 112 geographical coordinates of the dipole center, and the magnetic poles of the
 113 eccentric dipole. Details of the P_c computation based on the eccentric dipole
 114 model are given in the Appendix.

115 In order to account for the geomagnetic changes in the past, we make use
 116 of a paleomagnetic reconstruction over the last seven millennia provided by
 117 the CALS7K.2 model (Korte and Constable, 2005). The variations of the
 118 computed dipole moment M are shown in Fig. 1B for the last 6000 years.
 119 One can see that the general trend in the dipole moment was increasing: it
 120 was nearly doubled during the first half of the studied period, until about
 121 1000 BC, and remained at a high level of $(8\text{--}10) \times 10^{22}$ A m² after that.
 122 During that time, the magnetic axis was wandering quite essentially at the
 123 centennial scale (Korte and Constable, 2008; Usoskin et al., 2008) within the
 124 polar cap (geographical latitude above 80°).

125 Thus, CRII at a given location and time can be affected by variations
 126 of both the solar modulation of CR and the geomagnetic field, and their
 127 relative role varies over the Globe. Fig. 2 shows scatter plots of the CRII
 128 versus the two driving parameters, ϕ and M . One can see that, since there
 129 is no geomagnetic shielding in the polar region, polar CRII is totally defined
 130 by the solar modulation (panel A) and is independent of the geomagnetic

131 field (panel D). This relation is reversed in an equatorial region, where the
 132 CR variability is mostly defined by the magnetic dipole moment (panel F).
 133 The situation at mid-latitudes is more complicated. Both the geomagnetic
 134 dipole and solar changes play a role but none of them dominates (panels
 135 B and E). Moreover, migration of the geomagnetic axis becomes crucial at
 136 mid-latitudes (Kovaltsov and Usoskin, 2007; Usoskin et al., 2008). In order
 137 to illustrate the latter, we show in Fig. 1 also the CRII profiles at opposite
 138 longitudes (Greenwich and 180° meridians) at different latitudes. There is
 139 no longitudinal difference in the polar regions (panel C), and the maximum
 140 range of CRII variability between the Medieval maximum and the Maunder
 141 minimum is about 20%. Slowly varying difference at the equator (panel E) is
 142 caused by a changing offset in the dipole center with respect to the Earth's
 143 center with the range of variability being a factor of roughly 1.5. Variations
 144 of the CRII at mid-latitudes (panel D) are defined by all the factors: Before
 145 ca. 1500 BC, when the magnetic axis was not far from the geographical one,
 146 CRII was affected by both ϕ and M , but after that it was mostly dominated
 147 by the effect of the geomagnetic axis migration. This can be observed as
 148 the anti-phase variations of the CRII at opposite locations (solid and dotted
 149 curves) since 1400 BC. Thus, the millennial scale CRII variability can be
 150 roughly separated in three regions: Polar region, where the CRII is totally
 151 defined by the solar activity changes; Tropical region, where CRII is mostly
 152 dominated by changes in the geomagnetic field; Mid-latitude region, where
 153 both effects are equally important.

154 Figure 3 shows a geographical pattern of the millennial trends in CRII
 155 (defined as the slope of the best fit linear trend of the tropospheric CRII vari-
 156 ations in each location for the past 6800 years – see panels C–E in Fig. 1).
 157 Since the solar activity (Fig. 1A) and geomagnetic field strength (Fig. 1B)
 158 depict opposite millennial trends, the above three regions are clearly sepa-
 159 rated. CRII in polar regions (above 60–70° geographical latitude) shows a
 160 weak positive millennial trend (about 0.2% per century), corresponding to
 161 the overall decrease of the solar activity. On the other hand, strong negative
 162 CRII trend (up to -0.5% per century) is obtained around the (geomagnetic)
 163 equator, responding to the increasing geomagnetic moment. At the middle
 164 latitudes, the CRII remained at roughly the same level during the last mil-
 165 lennia. The globally averaged tropospheric CRII depicts a decreasing trend
 166 ($-0.2 \pm 0.03\%$ /century) over the past six millennia. We note that the pattern
 167 shown in Fig.3 would have been different if another time period was chosen.

168 Therefore, the global effect of CR upon Earth is defined, at this time scale

169 of several millennia, largely by changes in the geomagnetic field rather than
170 by solar variability.

171 **3. Possible climate implication**

172 In this section we compare long-term trends in CRII with some paleo-
173 climatic proxy as a simple statistical test of a possible relation between CR
174 variability and local climate on long time scales. Since the local/regional
175 variations are essential, we concentrate not on global indices but on some re-
176 gional paleoclimatic series, such as regional humidity/precipitation indices.
177 While global indices do not allow to clearly distinguish between direct and
178 indirect solar-terrestrial links (e.g., de Jager, 2005; Usoskin et al., 2005a),
179 the use of regional data may help in disentangling the effects, since CRII
180 has a geographical dependence different from that of direct solar influence
181 (insolation). Moreover, regional data are usually more or less homogeneous,
182 while global indices, obtained as spatial average/decomposition of the re-
183 gional data, may contain inhomogeneities and biases, especially when using
184 spatially sparse original data. In this study we emphasize long-term trends
185 in the data rather than detailed time variability of cosmic rays and terres-
186 trial parameters. Here we only aim to illustrate possible climate implications
187 of the long-term CRII variability by studying only statistical significance of
188 the relations without trying to support or refute any particular mechanism.
189 Neither do we pretend to provide a comprehensive analysis of all the exist-
190 ing climatic data sets, but we want to test the hypothesis of a link by one
191 example first.

192 We make use of an extensive database, related to the level of precipitation
193 – the global status of lakes around the world during the last 6–7 millennia.
194 This data set, available via the PMIP-2 Project GLSDB ([http://pmip2.lsce-
196 ipsl.fr/pmip2/synth/lakestatus.shtml](http://pmip2.lsce-
195 ipsl.fr/pmip2/synth/lakestatus.shtml)), contains the relative status of more
197 than 600 lakes around the world (Kohfeld and Harrison, 2000; Yu et al.,
198 2001; Harrison et al., 2003). Here we analyzed the present status of the lakes
199 compared to that 6800 calendar years ago (originally given as 6000 radio-
200 carbon years). Since the status of a lake is defined by the balance between
201 precipitation and evaporation, the wetter lake status generally correspond
202 to wetter/colder climate, and according to the adopted hypothesis on CR-
203 climate relation, to higher CRII (cf., e.g., Knudsen and Riisager, 2009). For
204 each lake, the relative status is quantified as $L = -2, -1, 0, 1, 2$, according
to whether the lake is presently much drier, drier, similar, wetter, and much

205 wetter, respectively, compared to that 6800 years ago. Here we consider
206 only general multi-millennial trends, ignoring detailed temporal comparison
207 of climatic and CR-related data, which has been studied, e.g., by Usoskin
208 and Kovaltsov (2008) for global and by Knudsen and Riisager (2009) for a
209 few regional climate indices.

210 Since the status of individual lakes may be not mutually independent
211 (closely located sites are expected to depict similar patterns), we averaged
212 the data available in relatively large geographical grid boxed (15° in longitude
213 $\times 10^\circ$ in latitude). Thus defined geographical pattern is shown in Fig. 4 with
214 colors ranging from blue (much drier) to red (much wetter). Lake data exists
215 for 84 out of 432 grid boxes, and the general pattern shows drying in Africa
216 and Asia, wetting in Northern America, and unsettled situation in South
217 America, Europe and Australia. This matrix of the relative lake status can
218 be quantitatively compared, in a statistical manner, to the CRII pattern.
219 The latter is represented by a map of the spatial distribution of the CRII
220 trend slope S (similar to that shown in Fig. 3) but computed for the same
221 geographical grid ($15^\circ \times 10^\circ$) as the lake status (Fig. 4). In each grid box, we
222 computed a product $P = S \times L$ of the lake status L (if available) and the CRII
223 trend slope S . According to the adopted CR-climate relation, we expect
224 an agreement between the two values (increasing CRII leads to wetter lake
225 status and vice versa). Therefore, we consider the parameter P as a measure
226 of the agreement between the two indices. A map of the distribution of the
227 agreement is shown in Fig. 5 (only the sign of the P is shown). General
228 agreement is observed over the entire Africa and a major fraction of Asia,
229 with a few spots in both Americas and in Australia. Disagreement is observed
230 in a region in Northern America and a few spots in South America, Near East
231 and Oceania. Europe, Alaska and Australia, i.e. the middle-to-high latitude
232 regions, remain uncertain. Visual inspection of the agreement does not allow
233 to evaluate its statistical significance – could it reflect a random pattern or
234 a causal link?

235 Accordingly, we have performed a statistical test of the result. The av-
236 erage value of $\langle P \rangle$ over all the 84 grid boxes is 0.18 ± 0.04 , i.e. significantly
237 positive, formally implying an agreement between the two sets of trends.
238 However, this value alone can be misleading since the lake status data ex-
239 ists mostly in the low-to-mid latitudes, where the CRII trend is dominantly
240 negative. Therefore, we estimate the significance of this result by a random
241 Monte-Carlo method. First we made an optimistic estimate, as follows. We
242 took the actual values of the lake status data L but assign them to randomly

243 selected grid boxes. Then new values of P^* were calculated for these grid
 244 boxes, using the actual CRII trends S there, and the average value $\langle P^* \rangle$
 245 was obtained. By repeating this procedure $N = 10000$ times, we obtained a
 246 distribution of $\langle P^* \rangle$. Finally, the number of simulations n with $|\langle P^* \rangle| > \langle P \rangle$
 247 gives an estimate of the significance α of the agreement between lake status
 248 and CRII trends (the probability that this agreement is due to a random
 249 coincidence without a causal link): $\alpha \equiv n/N$. This test yields very high
 250 significance $\alpha \approx 10^{-4}$. However, we consider this estimate as optimistic or
 251 overestimated, since it overlooks an important fact that the lake status data
 252 are distributed unevenly over the Globe. The lakes are located at the con-
 253 tinents, with a dominance of Africa-Eurasia, where CRII trends are mostly
 254 negative. Accordingly, an uncontrolled bias can be introduced in the above
 255 test, when the Monte-carlo simulated values are dropped randomly over the
 256 entire Globe. Next we consider a conservative test, when the L values are
 257 randomly shuffled inside the existing grid boxes, otherwise it is identical to
 258 the one described above. This test preserves the inhomogeneity of the data
 259 set. For this conservative test the estimated significance is $\alpha \approx 0.02$, indicat-
 260 ing that the probability of a random occurrence of the observed agreement
 261 between lake status and CRII trends is about 2%.

262 We note that both the above tests neglect a possible effect of the spatial
 263 (regional) correlation between the neighboring grid boxes (closely located
 264 lakes are expected to behave similarly). However, due to a large size of
 265 the grid boxes, this regional correlation is rather small (about 0.3) for the
 266 adjoining grid boxes and diminishes for larger scales.

267 4. Discussion and Conclusions

268 We have demonstrated that the long-term changes of the cosmic ray in-
 269 duced ionization in the low atmosphere are affected by two major factors:
 270 Solar variability, and geomagnetic field changes. While the former factor
 271 defines the CRII in the polar region, the latter dominates CRII variability
 272 in equatorial regions. CRII variability at middle latitudes is a result of an
 273 interplay between the two factors, which are both equally important. Fig. 3
 274 presents a geographical pattern of the long-term trend in the tropospheric
 275 CRII over the last 6000 years. We note that wandering of the geomagnetic
 276 dipole axis, which is crucially important in centennial changes of CRII at
 277 middle latitudes (Kovaltsov and Usoskin, 2007; Usoskin et al., 2008), is not a
 278 dominant factor at the multi-millennial time scale. Instead, the slow changes

279 of the geomagnetic dipole moment become very important in the tropics.
280 The long-term trend in regional CRII can be quite strong – up to a factor of
281 1.5 variations at the equator (see Fig. 1E). Interestingly, the trends have dif-
282 ferent slopes in different regions, viz. the CRII was increasing in polar areas
283 and decreasing in tropics. This fact makes it possible to perform a statistical
284 test of a relation between CRII and local/regional climate reconstructions.

285 The global effect of CR upon Earth is defined, at the studied time scale of
286 several millennia, largely by changes in the geomagnetic field rather than by
287 solar variability, which can lead to an unsettled effect of the apparent solar
288 variability on climate (e.g., Bard and Frank, 2006). On the other hand, this
289 may help in disentangling direct solar effects (e.g., via the irradiance) from
290 those caused by CR via the heliospheric modulation.

291 As an illustration of the possible climate implication we have compared
292 the reconstructed changes of the status of lakes around the world with the
293 CRII trend pattern for the last 6–7 millennia. The agreement between them
294 is significant – the probability of a random coincidence is estimated from
295 0.01% (optimistic estimate) to 2% (conservative estimate). At first glance,
296 even such a formally significant agreement may be casual not serving as an
297 evidence for a real link, because different trends in regional climate between
298 tropics and polar regions can be an intrinsic feature of the global climate sys-
299 tem. If so, detailed models of the climate dynamics throughout the Holocene,
300 using a general circulation model (GSM), would predict patterns comparable
301 with the map of lake status changes (Schmidt et al., 2004). Note however,
302 that results of such direct models, that include only the direct solar forc-
303 ing, did not yield general agreement with the observed lake status features
304 (Kohfeld and Harrison, 2000; Sawada et al., 2004). Therefore, it appears
305 plausible to think that the good agreement between CRII and lake status
306 patterns implies a real connection, viz. that changes in CRII may slightly
307 modulate the local climate. A similar conclusion has been drawn recently
308 by Knudsen and Riisager (2009) for China and Oman regional speleothem
309 precipitation data over the Holocene. However, this does not imply that
310 the other, direct, mechanisms via, e.g., solar insolation are less important.
311 Further studies using other climate parameters are necessary to investigate
312 particular mechanisms of the CRII climate relation, which is not attempted
313 here.

314 Concluding, we have demonstrated that:

- 315 • Long-term (multi-millennial) trends of the cosmic ray induced ioniza-

316 tion in the troposphere are defined not only by solar (i.e., covariant
317 with solar irradiance) changes but largely by changes of the geomag-
318 netic field.

319 • CRII variations are not spatially homogeneous but they depict a clear
320 geographical pattern. This is particularly important in tropical regions
321 and for global averaged data.

322 • Ionization in the polar region is mostly affected by the solar variability.

323 An analysis of spatio-temporal relation between the modelled ionization
324 trends and the lake level data as an example of the regional climate change
325 on the time scale of 6–7 millennia reveals a statistically significant correla-
326 tion between them, which appears better than the results of direct general
327 circulation modelling considering only the direct solar forcing.

328 This suggests that CRII may play a role in long-term regional climate
329 variations. The next step would be to include a geographical time-dependent
330 effect of CRII into general circulation models, in addition to all other known
331 effects, such as orbital forcing or solar irradiance variations, in an attempt
332 to model the corresponding observed patterns.

333 **Acknowledgements**

334 Supports from the Academy of Finland and the Finnish Academy of Sci-
335 ence and Letters Vilho, Yrjö and Kalle Väisälä Foundation are acknowledged.
336 GAK was partly supported by the Program of Presidium RAS N16-3-5.4. IM
337 acknowledges two grants (RNP.2.1.1.4166 “Geocosmos” and RNP.2.2.1.1.3836)
338 of the Russian Ministry of Education and Science.

339 **A. Computation of the geomagnetic cutoff rigidity**

340 Although computation of the geomagnetic cutoff rigidity in the eccentric
341 dipole approximation of the geomagnetic field is straightforward using vector
342 algebra and spherical geometry, it is lengthy and laborious. Since we are not
343 aware of a detailed published recipe for such a computation, we give its
344 essentials here.

345 In order to totally describe the geomagnetic field in the eccentric dipole
346 approximation (see full details in Fraser-Smith, 1987), one needs the first
347 eight Gauss coefficients of the magnetic field decomposition (for the centered

348 dipole, only 3 coefficients are sufficient). The eccentric dipole is assumed to
 349 posses the same magnetic dipole moment M and the same orientation of the
 350 magnetic axis as the centered dipole, but its center is displaced with respect
 351 to the Earth's center.

352 Let us consider a system of orthogonal Cartesian coordinates (x, y, z)
 353 with the origin at the Earth's center, so that the z -axis coincides with the
 354 Earth's rotational axis, the x -axis points to the crossing of the Greenwich
 355 meridian and the Equator, and the y -axis completes the right-hand system.
 356 In this reference frame let us define a system of spherical coordinates (r, θ, ψ)
 357 whose polar angle coincides with the z -axis.

The dipole moment is defined using the first three Gauss coefficients,
 g_1^0, g_1^1, h_1^1 , as

$$M = \frac{4\pi}{\mu_0} B_0 R_0^3, \quad (\text{A1})$$

where μ_0 is the free space magnetic permeability and R_0 is the mean radius
 of Earth, and

$$B_0^2 = (g_1^0)^2 + (g_1^1)^2 + (h_1^1)^2 \quad (\text{A2})$$

Let us denote vector

$$\mathbf{p} \left(-\frac{g_1^1}{B_0}; -\frac{h_1^1}{B_0}; -\frac{g_1^0}{B_0} \right)$$

as the direction of the dipole axis (the same for centered and eccentric dipole),
 and vector $\mathbf{d}(x_0; y_0; z_0)$ as the vector from the Earth's center to the center
 of eccentric dipole.

$$\begin{aligned} \frac{x_0}{R_0} &= \frac{L_1 - g_1^1 E}{3B_0^2}; \\ \frac{y_0}{R_0} &= \frac{L_2 - h_1^1 E}{3B_0^2}; \\ \frac{z_0}{R_0} &= \frac{L_0 - g_1^0 E}{3B_0^2}, \end{aligned} \quad (\text{A3})$$

where

$$\begin{aligned} L_0 &= 2g_1^0 g_2^0 + \sqrt{3} (g_1^1 g_2^1 + h_1^1 h_2^1) \\ L_1 &= -g_1^0 g_2^0 + \sqrt{3} (g_1^0 g_2^1 + g_1^1 g_2^2 + h_1^1 h_2^2) \\ L_2 &= -h_1^1 g_2^0 + \sqrt{3} (g_1^0 h_2^1 - h_1^1 g_2^2 + g_1^1 h_2^2) \\ E &= \frac{L_0 g_1^0 + L_1 g_1^1 + L_2 h_1^1}{4B_0^2}. \end{aligned}$$

Let us define \mathbf{r} ($R_0 \sin \theta \cos \psi$; $R_0 \sin \theta \sin \psi$; $R_0 \cos \theta$) as a vector from the Earth's center to the observational point with geographical co-latitude θ and longitude ψ on the surface. Let $\mathbf{R} = \mathbf{r} - \mathbf{d}$ be the vector from the center of the eccentric dipole to this observational point. The squared distance between the eccentric dipole center and the observational point is

$$R^2 = R_0^2 + d^2 - 2R_0(x_0 \sin \theta \cos \psi + y_0 \sin \theta \sin \psi + z_0 \cos \theta). \quad (\text{A4})$$

The geomagnetic co-latitude, i.e. the angle between the magnetic dipole axis and vector \mathbf{R} , $\theta_G = 90^\circ - \lambda_G$, can be defined as:

$$\begin{aligned} \cos \theta_G &= \frac{\mathbf{R} \cdot \mathbf{p}}{R p} = \\ &= \frac{1}{R B_0} [g_1^1(x_0 - R_0 \sin \theta \cos \psi) \\ &+ h_1^1(y_0 - R_0 \sin \theta \sin \psi) + g_1^0(z_0 - R_0 \cos \theta)] \end{aligned} \quad (\text{A5})$$

Finally, the vertical geomagnetic cutoff rigidity can be calculated using Störmer's equation (Eq. 2) as

$$Pc = 1.9 \cdot M \left(\frac{R_0}{R} \right)^2 \sin^4 \theta_G, \quad (\text{A6})$$

358 where Pc and M are given in GV and in 10^{22} A m², respectively. Thus
 359 computed cutoff rigidity has been used in the computations presented in this
 360 paper.

361 **References**

- 362 Arnold, F., 2008. Atmospheric Ions and Aerosol Formation. *Space Sci. Rev.*
 363 137, 225–239.
- 364 Bard, E., Frank, M., 2006. Climate change and solar variability: What's new
 365 under the sun? *Earth Planet. Sci. Lett.* 248, 1–2.
- 366 Bazilevskaya, G. A., Usoskin, I. G., Flückiger, E. O., Harrison, R. G., Des-
 367 orgher, L., Bütikofer, R., Krainev, M. B., Makhmutov, V. S., Stozhkov,
 368 Y. I., Svirzhevskaya, A. K., Svirzhevsky, N. S., Kovaltsov, G. A., 2008.
 369 Cosmic Ray Induced Ion Production in the Atmosphere. *Space Sci. Rev.*
 370 137, 149–173.

- 371 Bond, G., Kromer, B., Beer, J., Muscheler, R., Evans, M. N., Showers, W.,
372 Hoffmann, S., Lotti-Bond, R., Hajdas, I., Bonani, G., 2001. Persistent
373 Solar Influence on North Atlantic Climate During the Holocene. *Science*
374 294, 2130–2136.
- 375 Christl, M., Mangini, A., Holzkämper, S., Spötl, C., 2004. Evidence for a
376 link between the flux of galactic cosmic rays and Earth’s climate during
377 the past 200,000 years. *J. Atmosph. Sol.-Terr. Phys.* 66, 313–322.
- 378 Cooke, D., Humble, J., Shea, M., Smart, D., Lund, N., Rasmussen, I., Byr-
379 nak, B., Goret, P., Petrou, N., 1991. On cosmic-ray cut-off terminology.
380 *Nuovo Cimento C* 14, 213–234.
- 381 Courtillot, V., Gallet, Y., Le Mouél, J.-L., Fluteau, F., Genevey, A., Jan.
382 2007. Are there connections between the Earth’s magnetic field and cli-
383 mate? *Earth Planet. Sci. Lett.* 253, 328–339.
- 384 de Jager, C., 2005. Solar forcing of climate. 1: Solar variability. *Space Sci.*
385 *Rev.* 120, 197–241.
- 386 Dorman, L., 2004. *Cosmic Rays in the Earth’s Atmosphere and Underground.*
387 Kluwer Academic Publishers, Dordrecht, Netherlands.
- 388 Elsasser, W., Nay, E., Winkler, J., 1956. Cosmic-ray intensity and geomag-
389 netism. *Nature* 178, 1226–1227.
- 390 Foukal, P., Fröhlich, C., Spruit, H., Wigley, T., 2006. Variations in solar
391 luminosity and their effect on the earth’s climate. *Nature* 443, 161–166.
- 392 Fraser-Smith, A. C., 1987. Centered and eccentric geomagnetic dipoles and
393 their poles, 1600 - 1985. *Rev. Geophys.* 25, 1–16.
- 394 Gallet, Y., Genevey, A., Fluteau, F., 2005. Does Earth’s magnetic field sec-
395 ular variation control centennial climate change? *Earth Planet. Sci. Lett.*
396 236, 339–347.
- 397 Gallet, Y., Genevey, A., Le Goff, M., Fluteau, F., Ali Eshraghi, S., 2006.
398 Possible impact of the Earth’s magnetic field on the history of ancient
399 civilizations. *Earth Planet. Sci. Lett.* 246, 17–26.
- 400 Haigh, J. D., Blackburn, M., 2006. Solar Influences on Dynamical Coupling
401 Between the Stratosphere and Troposphere. *Space Sci. Rev.* 125, 331–344.

- 402 Haigh, J. D., Lockwood, M., Giampapa, M. S., 2005. The Sun, Solar Analogs
403 and the Climate. In: Rüedi, I., Güdel, M., Schmutz, W. (Eds.), Saas-Fee
404 Advanced Course 34: The Sun, Solar Analogs and the Climate. Springer
405 Verlag, Berlin.
- 406 Harrison, S. P., Kutzbach, J. E., Liu, Z., Bartlein, P. J., Otto-Bliesner, B.,
407 Muhs, D., Prentice, I. C., Thompson, R. S., 2003. Mid-Holocene climates
408 of the Americas: a dynamical response to changed seasonality. *Climate*
409 *Dynamics* 20, 663–688.
- 410 Hong, Y. T., Wang, Z. G., Jiang, H. B., Lin, Q. H., Hong, B., Zhu, Y. X.,
411 Wang, Y., Xu, L. S., Leng, X. T., Li, H. D., 2001. A 6000-year record
412 of changes in drought and precipitation in northeastern China based on a
413 $\delta^{13}\text{C}$ time series from peat cellulose. *Earth Planet. Sci. Lett.* 185, 111–119.
- 414 Hyodo, M., Biswas, D. K., Noda, T., Tomioka, N., Mishima, T., Itota,
415 C., Sato, H., Feb. 2006. Millennial- to submillennial-scale features of
416 the Matuyama-Brunhes geomagnetic polarity transition from Osaka Bay,
417 southwestern Japan. *J. Geophys. Res.* 111, B02103.
- 418 Kazil, J., Harrison, R. G., Lovejoy, E. R., 2008. Tropospheric New Particle
419 Formation and the Role of Ions. *Space Sci. Rev.* 137, 241–255.
- 420 Kazil, J., Lovejoy, E. R., Barth, M. C., O’Brien, K., 2006. Aerosol nucleation
421 over oceans and the role of galactic cosmic rays. *Atmosph. Chem. Phys.* 6,
422 4905–4924.
- 423 Kitaba, I., Iwabe, C., Hyodo, M., Katoh, S., Matsushita, M., 2009. High-
424 resolution climate stratigraphy across the matuyama-brunhes transition
425 from palynological data of osaka bay sediments in southwestern japan.
426 *Palaeogeograph. Palaeoclim. Palaeoecol.*, (in press).
- 427 Knudsen, M., Riisager, P., 2009. Is there a link between earth’s magnetic
428 field and low-latitude precipitation? *Geology* 37, 71–74.
- 429 Kohfeld, K., Harrison, S., 2000. How well can we simulate past cli-
430 mates? Evaluating the models using global palaeoenvironmental datasets.
431 *Quatern. Sci. Rev.* 19, 321–346.
- 432 Korte, M., Constable, C., 2005. Continuous geomagnetic field models for the
433 past 7 millennia: 2. CALS7K. *Geochem., Geophys., Geosys.* 6, Q02H16.

- 434 Korte, M., Constable, C., 2008. Spatial and temporal resolution of millennial
435 scale geomagnetic field models. *Adv. Space Res.* 41, 57–69.
- 436 Kovaltsov, G. A., Usoskin, I. G., 2007. Regional cosmic ray induced ionization
437 and geomagnetic field changes. *Adv. Geosci.* 13, 31–35.
- 438 Kudela, K., Usoskin, I. G., 2004. On Magnetospheric Transmissivity of Cos-
439 mic Rays. *Czec. J. Phys.* 54, 239–254.
- 440 Marsh, N., Svensmark, H., 2003. Solar Influence on Earth’s Climate. *Space*
441 *Sci. Rev.* 107, 317–325.
- 442 Mironova, I. A., Desorgher, L., Usoskin, I. G., Flückiger, E. O., Bütikofer,
443 R., 2008. Variations of aerosol optical properties during the extreme solar
444 event in January 2005. *Geophys. Res. Lett.* 35, L18610.
- 445 Niggemann, S., Mangini, A., Mudelsee, M., Richter, D. K., Wurth, G., 2003.
446 Sub-Milankovitch climatic cycles in Holocene stalagmites from Sauerland,
447 Germany. *Earth Planet. Sci. Lett.* 216, 539–547.
- 448 Pallé, E., Butler, C. J., O’Brien, K., 2004. The possible connection between
449 ionization in the atmosphere by cosmic rays and low level clouds. *J. At-*
450 *mosph. Solar-Terr. Phys.* 66, 1779–1790.
- 451 Sawada, M., Viau, A. E., Vettoretti, G., Peltier, W. R., Gajewski, K., 2004.
452 Comparison of North-American pollen-based temperature and global lake-
453 status with CCCma AGCM2 output at 6ka. *Quatern. Sci. Rev.* 23, 225–
454 244.
- 455 Scherer, K., Fichtner, H., Borrmann, T., Beer, J., Desorgher, L., Flückiger,
456 E., Fahr, H.-J., Ferreira, S. E. S., Langner, U. W., Potgieter, M. S., Heber,
457 B., Masarik, J., Shaviv, N., Veizer, J., 2006. Interstellar-Terrestrial Re-
458 lations: Variable Cosmic Environments, The Dynamic Heliosphere, and
459 Their Imprints on Terrestrial Archives and Climate. *Space Sci. Rev.* 127,
460 327–465.
- 461 Schmidt, G. A., Shindell, D. T., Miller, R. L., Mann, M. E., Rind, D., 2004.
462 General circulation modelling of Holocene climate variability. *Quatern. Sci.*
463 *Rev.* 23, 2167–2181.

- 464 Smart, D. F., Shea, M. A., Flückiger, E. O., 2000. Magnetospheric Models
465 and Trajectory Computations. *Space Sci. Rev.* 93, 305–333.
- 466 Tinsley, B. A., 2008. The global atmospheric electric circuit and its effects
467 on cloud microphysics. *Rep. Prog. Phys.* 71, 066801.
- 468 Usoskin, I., Schüssler, M., Solanki, S., Mursula, K., 2005a. Solar activity,
469 cosmic rays, and earth’s temperature: A millennium-scale comparison. *J.*
470 *Geophys. Res.* 110 (A10).
- 471 Usoskin, I. G., Alanko-Huotari, K., Kovaltsov, G. A., Mursula, K., 2005b.
472 Heliospheric modulation of cosmic rays: Monthly reconstruction for 1951–
473 2004. *J. Geophys. Res.* 110, A12108.
- 474 Usoskin, I. G., Desorgher, L., Velinov, P., Storini, M., Flückiger, E. O.,
475 Bütikofer, R., Kovaltsov, G. A., 2009. Ionization of the earth’s atmosphere
476 by solar and galactic cosmic rays. *Acta Geophys.* 57, 88–101.
- 477 Usoskin, I. G., Gladysheva, O. G., Kovaltsov, G. A., 2004. Cosmic ray-
478 induced ionization in the atmosphere: spatial and temporal changes. *J.*
479 *Atmos. Solar-Terr. Phys.* 66, 1791–1796.
- 480 Usoskin, I. G., Korte, M., Kovaltsov, G. A., 2008. Role of centennial geo-
481 magnetic changes in local atmospheric ionization. *Geophys. Res. Lett.* 35,
482 L05811.
- 483 Usoskin, I. G., Kovaltsov, G. A., 2004. Long-term solar activity: Direct and
484 indirect study. *Solar Phys.* 224, 37–47.
- 485 Usoskin, I. G., Kovaltsov, G. A., 2006. Cosmic ray induced ionization in the
486 atmosphere: Full modeling and practical applications. *J. Geophys. Res.*
487 111, D21206.
- 488 Usoskin, I. G., Kovaltsov, G. A., 2008. Cosmic rays and climate of the Earth:
489 Possible connection. *C. R. Geosci.* 340, 441–450.
- 490 Usoskin, I. G., Solanki, S. K., Kovaltsov, G. A., 2007. Grand minima and
491 maxima of solar activity: new observational constraints. *Astron. Astro-*
492 *phys.* 471, 301–309.

- 493 Usoskin, I. G., Voiculescu, M., Kovaltsov, G. A., Mursula, K., 2006. Cor-
494 relation between clouds at different altitudes and solar activity: Fact or
495 Artifact? *J. Atmosph. Sol.-Terr. Phys.* 68, 2164–2172.
- 496 Van Geel, B., Raspopov, O., Renssen, H., Van der Plicht, J., Dergachev, V.,
497 Meijer, H., 1999. The role of solar forcing upon climate change. *Quatern.*
498 *Sci. Rev.* 18, 331–338.
- 499 Versteegh, G., 2005. Solar forcing of climate. 2: Evidence from the past.
500 *Space Sci. Rev.* 120, 243–286.
- 501 Voiculescu, M., Usoskin, I. G., Mursula, K., 2006. Different response of clouds
502 to solar input. *Geophys. Res. Lett.* 33, L21802.
- 503 Webber, W., 1962. Time variations of low rigidity cosmic rays during the
504 recent sunspot cycle. In: Wilson, J., Wouthuysen, S. (Eds.), *Progress in*
505 *Elementary Particle and Cosmic Ray Physics*,. Vol. 6. North Holland, Am-
506 *sterdam*, pp. 77–243.
- 507 Xiao, J., Nakamura, T., Lu, H., Zhang, G., 2002. Holocene climate changes
508 over the desert/loess transition of north-central China. *Earth Planet. Sci.*
509 *Lett.* 197, 11–18.
- 510 Yu, G., Harrison, S., Xue, B., 2001. Lake status records from china: Data
511 base documentation. Technical Reports 4, Max-Planck-Institut fr Biogeo-
512 *chemie*, Germany.

Figure 1: Time profiles for the last 6000 years (all data are averaged over calendar centuries). Panel A: Cosmic ray modulation potential ϕ (in MV), reconstructed from the cosmogenic ^{14}C data by Usoskin et al. (2007). Panel B: Geomagnetic dipole moment M (in 10^{22} A m²), computed from the CALS7K.2 model (Korte and Constable, 2005, 2008). Panel C: Normalized cosmic ray induced ionization in the middle troposphere (residual atmospheric depth 500 g/cm² or the altitude of about 5.8 km), computed using the CRAC:CR11 model (Usoskin and Kovaltsov, 2006, - see text for details) for the polar region (72°N 0°E). Panel D: The same as panel C but for mid-latitudes (45°N 0°E - solid line, 45°N 180°E - dotted line). Panel E: The same as panel C but for the equator (0°N 0°E - solid line, 0°N 180°E - dotted line). Grey lines depict the best-fit linear trend, computed for the solid curve, in each panel.

Figure 2: Dependence of the normalized tropospheric cosmic ray induced ionization on the modulation parameter ϕ (panels A–C) and the geomagnetic dipole moment M (panels D–F) for the last 6000 years. Top, middle and bottom row panels correspond to the polar, mid-latitude and equatorial regions, respectively.

Figure 3: Spatial pattern ($5^\circ \times 5^\circ$ grids) of the millennial trend in tropospheric cosmic ray induced ionization for the last 6800 years (see text for definition). Color scale to the right represents the slope of the trend in %/century.

Figure 4: Spatial pattern of the millennial trend in the lake status (see text for definition). Red, yellow, white, light blue and blue colors correspond to much wetter, wetter, no change, drier and much drier present status, respectively, of the lakes compared to that 6800 BP. Regions without data of the lake status are filled in grey.

Figure 5: The agreement P (see text for definition) between millennial trends in the tropospheric cosmic ray induced ionization and in the lake status. Black and white rectangles correspond to regions of agreement and disagreement, respectively. Hatched rectangles depict regions with unsettled relation ($|P| < 0.1$). Regions without data of the lake status are filled in grey.

Figure 1

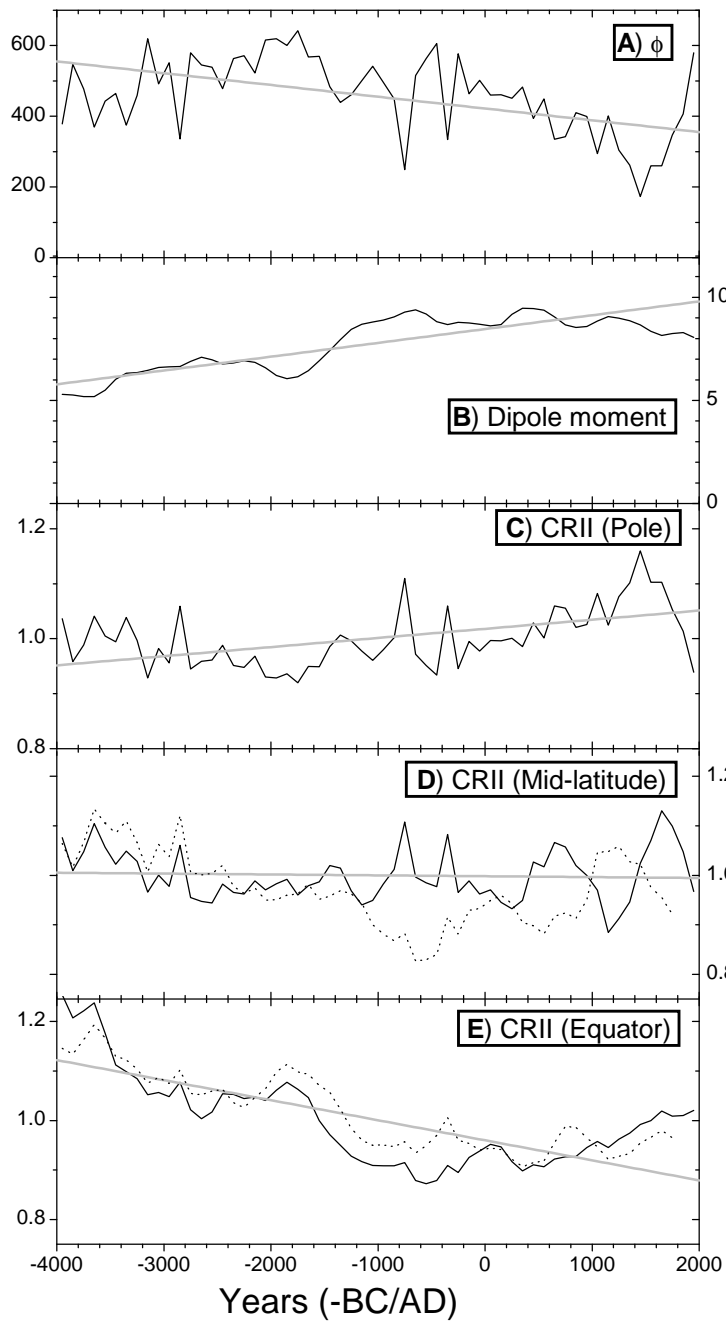


Figure 2

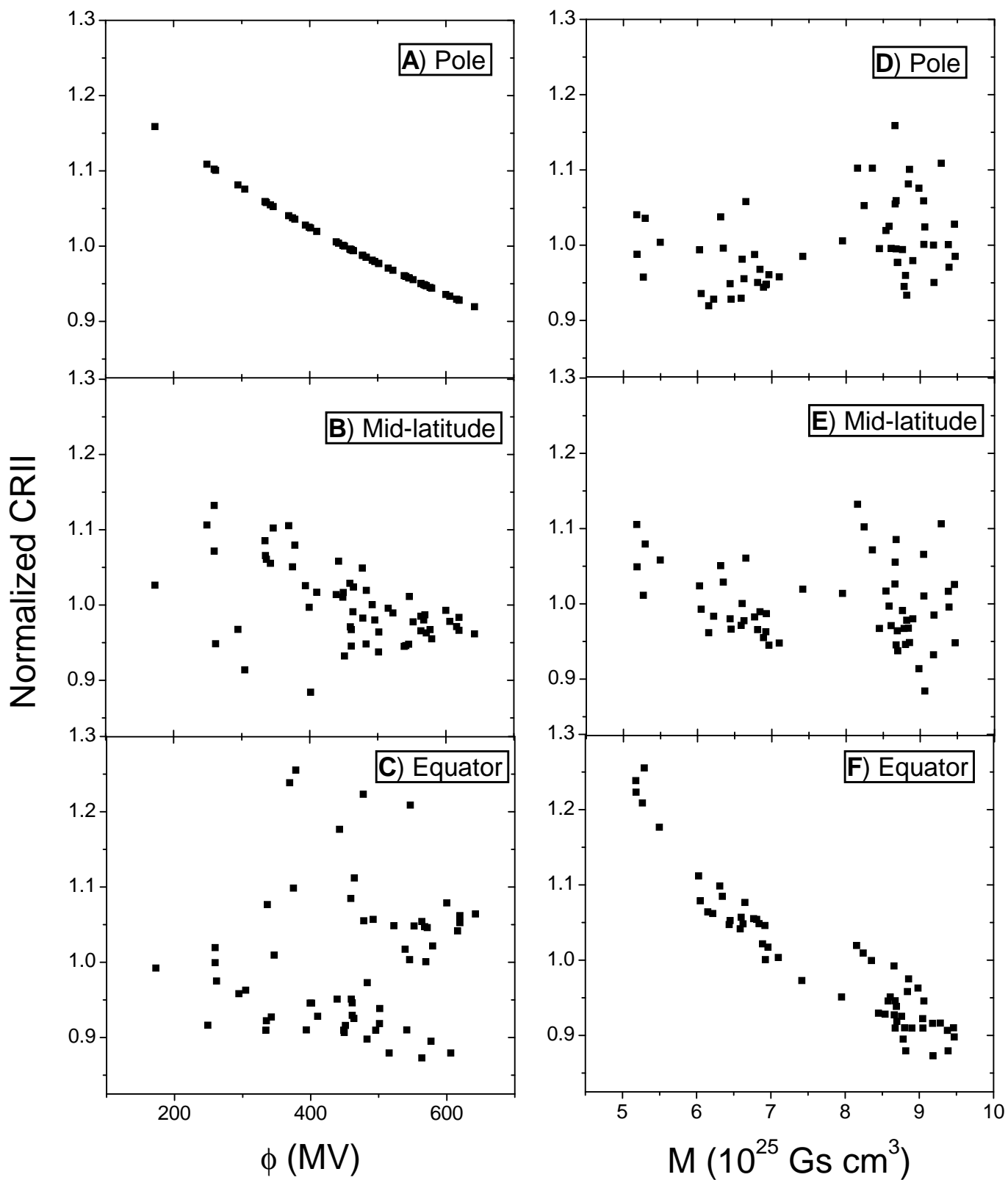


Figure 3

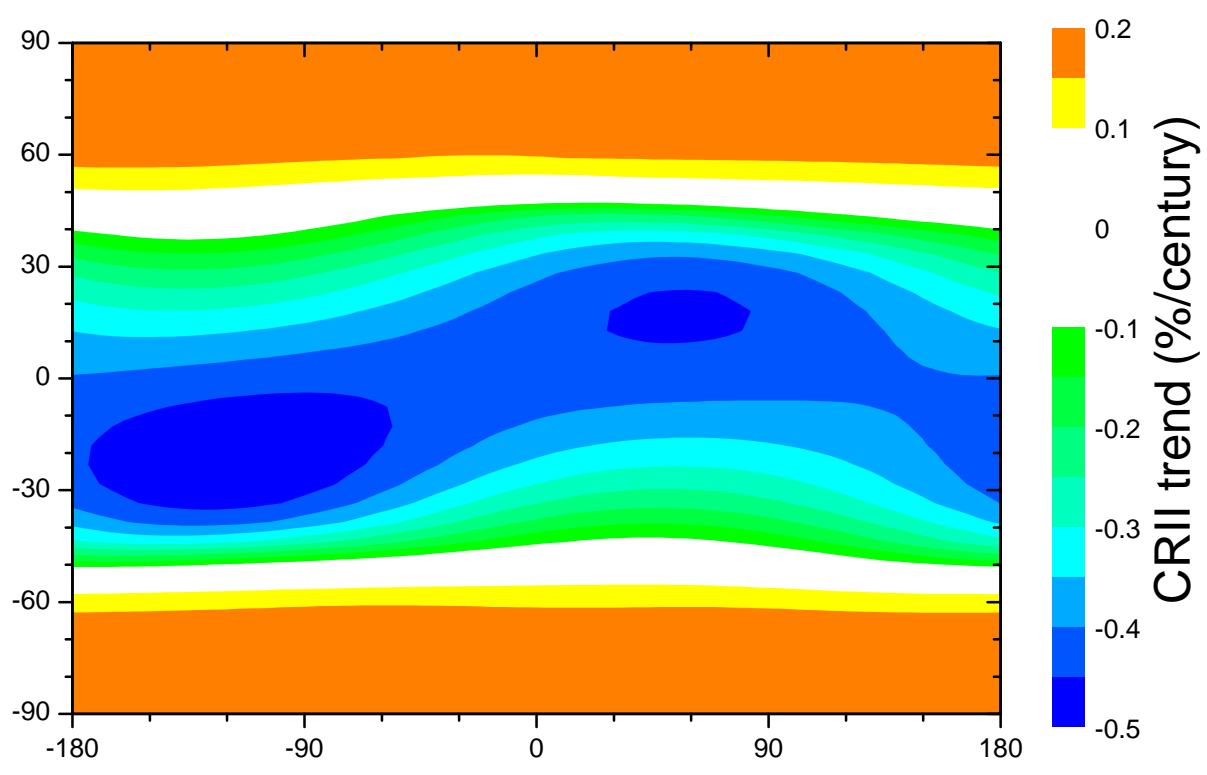


Figure 4

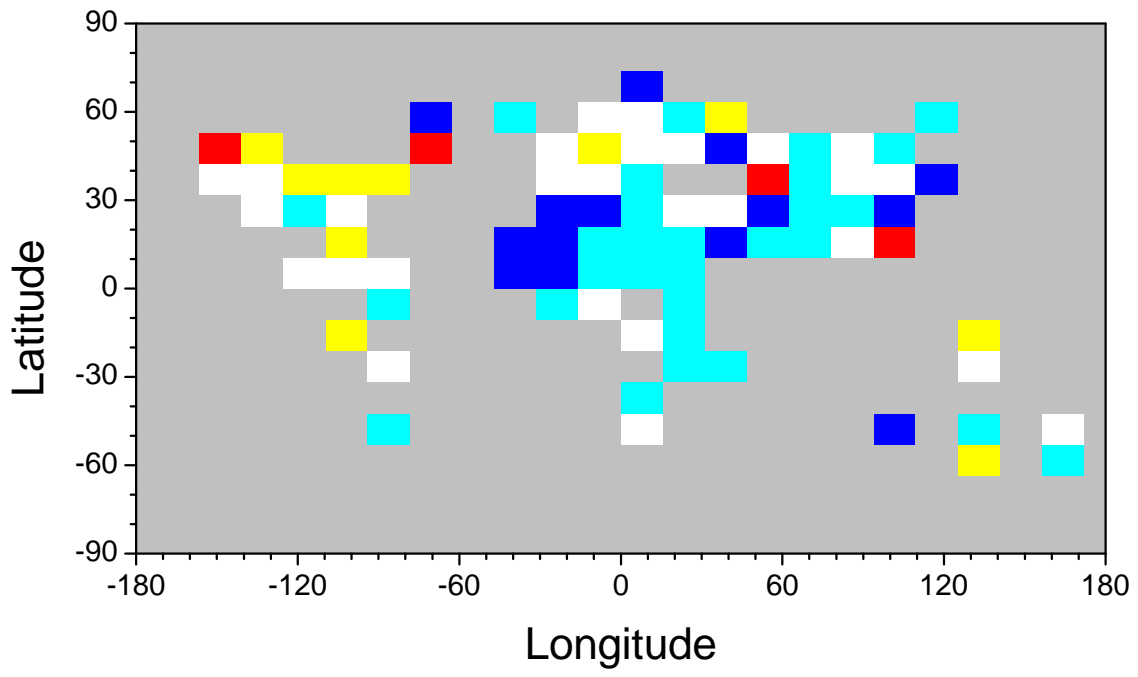


Figure 5

